Plasmonically-enhanced ultrasensitive epitope specific serologic assay for COVID-19

Zheyu Wang[1], Jeremiah J. Morrissey[2, 3, *], Lin Liu[1], Yixuan Wang[1], Qingjun Zhou[1], Rajesh R. Naik[4, *], Srikanth Singamaneni[1, 3, *]

[1]Department of Mechanical Engineering and Materials Science, Institute of Materials Science and Engineering, Washington University in St. Louis, St Louis, MO, 63130, USA.

[2]Department of Anesthesiology, Division of Clinical and Translational Research, Washington University in St. Louis, St. Louis, MO, 63110, USA

[3]Siteman Cancer Center, Washington University School of Medicine, St. Louis, MO, 63110, USA

[4]711th Human Performance Wing, Air Force Research Laboratory, Wright Patterson Air Force Base, Dayton, OH, 45433, USA

*To whom correspondence should be addressed: singamaneni@wustl.edu (SS) and morrisseyjj@wustl.edu (JJM)

Abstract:

Severe acute respiratory syndrome coronavirus-2 (SARS-CoV-2) has rapidly spread and resulted in global pandemic of COVID-19. Although IgM / IgG serology assay has been widely used, with the entire spike or nucleocapsid antigens, they only indicate the presence or absence of antibodies against these proteins, but not specific to the neutralization antibodies, therefore providing coarse only generic information about infection stage and possible future immune protection. Novel technologies enabling easy-to-use and sensitive detection of multiple specific antibodies simultaneously will facilitate precise diagnosis of infection stages, prediction of clinical outcomes, and evaluation of future immune protection upon vial exposure or vaccination. Here, we demonstrate a rapid and ultrasensitive quantification method for epitope-specific antibodies, including different isotypes and subclasses, in a multiplexed manner. Using an ultrabright fluorescent nanolabel, plasmonic-fluor, this novel assay can be completed in 20 minutes and, more importantly, the LOD of the plasmon-enhanced immunoassay for SARS-CoV-2 antibodies is as much as 100-fold lower compared to the assays relying on enzymatic amplification of colorimetric signal. Using convalescent patient plasma, we demonstrate that this biodetection method reveals the patient-to-patient variability in immune response as evidenced by the variations in whole protein and epitope-specific antibodies. This cost-effective, rapid and ultrasensitive plasmonically-enhanced multiplexed epitope-specific serological assay has the potential to be broadly employed in the detection of specific antibodies, which may benefit to advance epidemiology studies, and enable improvement of the clinical outcomes, and prediction of the future protection against the SARS-CoV-2.

Introduction：

Severe acute respiratory syndrome coronavirus-2 (SARS-CoV-2) has been unprecedentedly threatening the public health worldwide. As of May 2021, more than 160 million cases of coronavirus disease 2019 (COVID-19) have been reported, resulting in over 3.4 million deaths.[1] Although the fast development and administration of vaccines have mitigated the pandemic, it remains important to achieve early diagnosis and improve treatment of COVID-19. Moreover, rapidly spreading SARS-CoV-2 variants have emerged as one of the new challenges as they may jeopardize the efficacy of vaccines and current monoclonal antibodies or antibodies in convalescent plasma for prototype SARS-CoV-2.[2-3] These monoclonal or polyclonal antibodies block virus interaction by inhibiting their attachment to susceptible cells and/or block proteolytic cleavage of the virus spike protein essential for penetration into the target cells. Antibodies that recognize and attach to linear epitopes on the SARS-CoV-2 spike protein S1 and/or S2 regions provide “correlates of protection” to viral infection[4] and can functionalize gold nanoparticles for detection of epitope-specific antibodies[5]. These “correlate” antibodies, along with antibodies against the receptor binding domain (RBD) of the spike protein, help to neutralize the SARS-CoV-2 virus from infecting susceptible cells. Stepping into the post-pandemic era, there is a dire need for novel technologies, which will rapidly and precisely diagnose symptomatic and asymptomatic disease, and predict the infection course, reducing the mortality of COVID-19 patients, as well as evaluate the persistence of acquired immunity against prototypical SARS-CoV-2 and its variants upon vaccination.

Conventional single-plex serology assays employ pristine SARS-CoV-2 spike (S) protein, the receptor binding domain (RBD) of the spike protein or nucleocapsid (N) protein as recognition elements (*i.e.* as antigen baits) to capture target antibodies.[6-7] Despite its simplicity and low cost, conventional serological tests only provide coarse information about viral exposure history, infection stage and are variable in predicting neutralizing activity.[8] This limitation primarily stems from the use of whole proteins or even regions of proteins such as the 223 amino acid RBD or the 301 amino acid N-terminal domain (NTD) of the S protein as baits, where the results only demonstrate overall antibody reaction, which are prone to interference from other coronaviruses owing to the cross reactivity and

lack details about informative antibody subclass. Detection and quantification of antibodies that bind to specific epitopes within a whole protein or a domain requires highly sensitive detection modalities. With deeper understanding of humoral response, recent studies have discovered that antibodies towards different epitopes may exhibit polarized functions, while part of them will neutralize the interactions between virus and host cells, others may inversely exacerbate patient outcome due to the antibody-dependent enhancement (ADE) effect, correlating with the severity of COVID-19.[9-11] Therefore, early detection and identification of antibodies targeting precise epitopes will improve the diagnosis and help determine the future protection afforded to patients suffering from mild to severe COVID-19. More importantly, this information can be employed to evaluate and predict the clinical efficacy of vaccines against SARS-CoV-2 including both prototype and variants.

In this work, we demonstrate the integration of plasmonic-fluor, an ultrabright fluorescent nanolabel, with SARS-CoV-2 serology assays to achieve the ultrasensitive detection of epitope-specific antibody isotype and subclass in both a microtiter whole well format and a spatially-multiplexed manner measuring two different epitopes within a single microtiter well. Contrary to the conventional serological tests relying on whole protein or large protein domains, we employed BSA-peptide encoding specific epitope sequences from SARS-CoV-2 spike protein as the antigen and plasmonic-fluor as an ultrabright and highly specific fluorescent nanolabel. Plasmonic-fluor has been reported to achieve more than 6000 times brighter florescence signal compared to the conventional fluorophores. Plasmonic-fluor improved the sensitivity up to three orders of magnitude for numerous bioanalytical techniques, including immunomicroarrays, fluorescence linked immunosorbent assay (FLISA), bead-based fluoroimmunoassays and flow cytometry.[12] Here, we demonstrate that application of plasmonic-fluor results in an ultrasensitive serology assay, which can be employed for the detection and quantification of SARS-CoV-2 epitope-specific antibodies in convalescent patient plasma in both biomedical research and clinical diagnosis (Figure 1).

Experimental section:

Convalescent plasma samples: Convalescent plasma samples utilized in this study were obtained from the Washington University School of Medicine's COVID-19 biorepository, which is supported by: the Barnes-Jewish Hospital Foundation; the Siteman Cancer Center grant P30 CA091842 from the National Cancer Institute of the National Institutes of Health; and the Washington University Institute of Clinical and Translational Sciences grant UL1TR002345 from the National Center for Advancing Translational Sciences (NCATS) of the National Institutes of Health (NIH). This repository was developed and is maintained by Jane O'Halloran, MD, PhD; Charles Goss, PhD, and Phillip Mudd, MD, PhD. All patient samples used in this study were obtained under approval of IRB 202004097 from the Washington University Institutional Review Board. The content is solely the responsibility of the authors and does not necessarily represent the view of the NIH.

Synthesis of plasmonic fluor: Plasmonic-fluor was synthesized according to a previously reported procedure and prepared by Auragent Bioscience LLC.[13]

Synthesis of AuNRs: For plasmonic-fluor 800, AuNRs (LSPR wavelength ~760 nm) were prepared through a seed-mediated method.[14] Briefly, to prepare seed solution, 600 μl of 10 mM ice-cold $NaBH_4$ solution (Sigma-Aldrich, 71321) was added to a mixture solution comprised of 250 μl of 10 mM $HAuCl_4$ (Sigma-Aldrich, 520918) and 9.75 ml of 100 mM hexadecyltrimethylammonium bromide (CTAB, Sigma-Aldrich, H5882), under vigorous stirring at room temperature. The color change of the mixture solution from yellow to brown indicates the formation of seed crystals and the solution was allowed to age in dark for one hour before further usage. To synthesize the gold nanorods, the growth solution was first prepared through sequential addition of CTAB (100 mM, 38 ml), $AgNO_3$ (10 mM, 0.5 ml) (Sigma-Aldrich, 204390), $HAuCl_4$ (10 mM, 2 ml), ascorbic acid (0.1 M, 0.22 ml) (Sigma-Aldrich, A92902) and HCl (1 M, 0.9 ml) (Sigma-Aldrich, H9892). Subsequently, 50-fold diluted seed solution was added into the growth solution and left undisturbed overnight in dark. AuNRs were collected by centrifugation at 6000 rpm to remove the supernatant and redispersed in nanopure water for further use.

Conjugation of Biotin and Cy7.5 dye onto BSA: Bovine serum albumin (BSA) was sequentially conjugated with biotin and Cy7.5 dye via EDC/NHS chemistry. First, 2 mg pf

NHS-PEG_4-Biotin (Thermo Scientific, 21330) was added into 2.2 ml of 5 mg/ml BSA (Sigma-Aldrich, A7030) in 1X PBS. After reaction for one hour, BSA-Biotin conjugation was purified through a desalting column (Thermo Scientific, 89892, 7000 MWCO). To conjugate BSA with Cy7.5 dye, 100 μl of 1 M potassium phosphate dibasic solution (K_2HPO_4, Sigma Aldrich, P3786) was added into 1 ml BSA-Biotin solution to raise the pH above 9. Subsequently, 25 μl of 4 mg/ml NHS-Cy7.5 (Lumiprob, 16020) was added to the mixture, followed by two-hour incubation at room temperature. BSA-biotin-Cy7.5 was purified through a desalting column pre-equilibrated with nanopure water.

Synthesis of plasmonic-fluor: To prepare plasmonic fluor-800, AuNRs (LSPR wavelength around 760 nm), as nanoantennas, were first coated with a thin layer of polymer to avoid fluorescence quench. Briefly, 5 μl of (3-mercaptopropyl)trimethoxysilane (MPTMS, Sigma-Aldrich, 175617) was added into 5 ml of AuNRs solution (extinction around 2), followed by one hour incubation at 24 °C. MPTMS modified AuNRs were collected through centrifugation at 6000 rpm for 10 minutes and redispersed in 1 mM CTAB solution. 2 μl APTMS and 2 μl TMPS were sequentially added into the MPTMS modified AuNRs solution to form the polymer layer. Finally, AuNR-polymer were collected through three centrifugations at 6000 rpm for 10 minutes and concentrated into a final volume of 10 μl.

Next, to coat BSA-Biotin-Cy7.5 conjugate around AuNR-polymer, 1 μl of 20 mg/ml citric acid (Alfa Aesar, 36664) was added into 100 μl 4 mg/ml BSA-biotin-Cy7.5 solution. Concentrated AuNR-polymer were subsequently added into the mixture solution and sonicated for 20 minutes in dark. Coated nanostructures were further collected by centrifugation at 4000 rpm for 5 minutes before incubation with 500 μl of 0.4 mg/ml BSA-Biotin-Cy7.5 at pH 10 nanopure water for at least 3 days in 4 °C. The nanostructures were washed through 4 times centrifugation at 6000 rpm for 10 minutes using pH 10 water and redisperse in 1% BSA 1X PBS solution before use.

Fluorescence enhancement with plasmonic fluor: The schematic of test procedure was illustrated in Supplementary Figure S1. Specifically, 100 μl 50 ng/ml BSA-biotin was first incubated with 96 well plate for 10 minutes. The plate was subsequently washed by 1X PBS with 0.05% Tween-20 (Sigma Aldrich, P2287) (PBST) and blocked with 3% BSA 1X PBS solution for one hour. Streptavidin-CW800 (1 μg/ml) was added and incubated for

10 minutes, followed by three times washing with PBST. The plate was further incubated with 76 pM plasmonic fluor-800 in 1% BSA solution. After washing, fluorescence signal before and after incubation of plasmonic fluor were recorded using LI-COR CLx fluorescence scanner with following parameters: channel: 800, laser power: L2, resolution: 21 μm, height: 4 mm.

Conjugation of SARS-CoV-2 epitopes on BSA. Peptides with the sequence of epitopes were ordered from GenScript according to the sequence reported in previous paper. [10] To conjugate peptide with BSA, an amino acid spacer, cysteine-glycine-glycine-glycine (CGGG), was designed to be the end group at the N-terminal. The complete sequence is shown below:

Peptide 1: CGGGTESNKKFLPFQQFGRDIA

Peptide 2: CGGGPSKPSKRSFIEDLLFNKV

The obtained peptides were conjugated with BSA through sulfosuccinimidyl-4- (N-maleimidomethyl) cyclohexane – 1 - carboxylate (Sulfo-SMCC, Thermo Scientific, A39268). First, to conjugate linkers with BSA, sulfo-NHS esters from the linker were reacted with amine groups on BSA. Specifically, 0.5 mg sulfo-SMCC was added to 1 ml of BSA (Sigma-Aldrich, A7030) solution (3 mg/ml in 1X PBS, 1.2 mM EDTA, pH 7.2) and incubate for 30 minutes at room temperature. Conjugated BSA were purified through the desalting column (7000 MWCO, Thermo Scientific, 89890) pre-equilibrated with 1X PBS, 1.2 mM EDTA. To conjugate the peptides, maleimide groups from conjugated BSA were reacted with sulfhydryl groups from peptides through Michael addition. 2 mg peptides were added to 500 μl BSA conjugate solution and incubated for 60 minutes at room temperature. The BSA-peptide was subsequently purified using a desalting column pre-equilibrated with 1X PBS.

Enzyme-linked immunosorbent assay for SARS-CoV-2 antibody detection (within 20 minutes)

The detailed information of antigens, targeting antibody and secondary antibody in various types of antibody detection assay are listed in Table S1. Generally, eight-well high binding polystyrene ELISA strips (Thermo Scientific, 15031) were pre-coated with 100 μl

of antigen solution at a concentration of 2 µg/ml in PBS overnight at 4 °C. The wells were washed with PBST and blocked with 350 µl of 3% BSA for 1 hour at room temperature followed. After washing, wells were incubated with commercialized standard samples or serial diluted patient plasma samples in PBST for 5 minutes, followed by washing and incubation of secondary antibody for 5 minutes. Streptavidin-horseradish peroxidase (HRP) (R&D Systems, 893975) were subsequently incubated for 5 minutes. 100 µl of substrate solution (1:1 mixture of color reagent A (H_2O_2) and color reagent B (tetramethylbenzidine)) (R&D Systems, DY999) was incubated and stopped by 50 µl 2N Sulfuric acid (R&D Systems, DY994) after 5 minutes. Optical density of each well was measured using microtiter plate reader set at 450 nm.

Fluorescence or plasmonic fluor-enhanced immunosorbent assay for SARS-CoV-2 antibody detection (within 20 minutes)

The FLISA were implemented using the similar approach as the standard enzymatic immunoassay, except that conventional enzyme mediated reporters were replaced by streptavidin-CW800 (LICOR, 926-32230). In case of p-FLISA, the wells were further washed with PBST for three times and 100 µl plasmonic fluor were subsequently added and incubated for 5 minutes. After washing, the wells were imaged using LI-COR CLx fluorescence imager with the following scanning parameters: laser power ~L2; resolution ~21 µm; channel 800; height 4 mm. For the detection of epitope specific antibody, the fluorescence intensity of albumin specific antibody in each plasma sample was subtracted as background to achieve the pristine intensity of SARS-CoV-2 specific antibody.

Plasmonic fluor-enhanced multiplexed detection of epitope specific SARS-CoV-2 antibody. The multiplex detection was achieved by spatial blotting of different BSA-peptide conjugates within the same well of microtiter plate. Specifically, a 2-µl droplet of 4 µg/ml BSA-peptide 1 conjugates in 1X PBS with 10% glycerol were carefully blotted on the left part of the well, followed by another droplet of BSA-peptide 2 conjugates on the right. The microtiter plate was then sealed and incubated in 4 °C overnight, followed by blocking with 300 µl of reagent diluent (1X PBS containing 3% BSA, 0.2 µm filtered). The remaining steps were same as indicated above. For the detection of epitope specific antibody, the fluorescence intensity of albumin specific antibody in each plasma sample

(intensity in the rest part of the well) was subtracted as background to achieve the pristine intensity of SARS-CoV-2 specific antibody. To determine the titer of epitope specific antibody in each sample, a cut-off value equals to mean fluorescence signal acquired from healthy control plus three times of standard deviation.

Material characterization: TEM images were obtained using a JEOL JEM-2100F field emission instrument. To prepare the TEM sample, a drop of aqueous solution was dried on a hydrophilic carbon-coated grid. SEM images were obtained using a FEI Nova 2300 field-emission SEM at an accelerate voltage of 10 KV. The extinction spectra of plasmonic nanoparticles were obtained using Shimadzu UV-1800 spectrophotometer. Fluorescence mappings were obtained using LI-COR Odyssey CLx imaging system.

Results and discussion

Design and synthesis of Plasmonic-fluor

Conventional serological tests detect antibodies via a sandwich enzyme-linked immunosorbent assay (ELISA). The enzymatic reaction results in the formation of soluble colored products in an antibody concentration-dependent manner. While routinely employed, this approach is not suitable for the fast, sensitive, and multiplexed detection of epitope-specific antibody, due to (1) relatively low sensitivity, making the fast quantification of low abundant antibody challenging, and (2) the soluble nature of the colored product, precluding the possible spatially- multiplexed detection. Therefore, existing technologies for COVID-19 are limited to the detection of antibodies against the whole S protein, RBD domains or N proteins, which only provide incomplete information with considerable heterogeneity and have limited capability to detect and quantify low IgG titers.[15-16] To overcome this challenge, we used a fluorescence-linked immunosorbent assay (FLISA) that relies on plasmonic-fluor as an ultrabright and highly specific fluorescent label (Figure 2A). Plasmonic-fluor is composed of a gold nanorod (AuNR) coated with fluorophores (800CW) and a universal biorecognition element (biotin).[13] Bovine serum albumin (BSA) is employed as a scaffold to assemble all functional elements and to minimize non-specific protein binding. A siloxane copolymer spacer

layer between the AuNRs and the fluorophores is employed to avoid metal-induced fluorescence quenching. The relatively narrow longitudinal localized surface plasmon resonance (LSPR) wavelength of the plasmonic-fluors indicated the colloidal stability of the nanolabels (Figure 2B). Binding of the plasmonic-flour-800CW to streptavidin-CW800 coated on microtiter plates resulted in a nearly 1500-fold enhancement of ensemble fluorescence intensity (Figure 2C).

Rapid detection of antibodies against SARS-CoV-2

To investigate the applicability of plasmonic-fluor as an ultrabright nanolabel in a fast SARS-CoV-2 serological assay, we use anti SARS-CoV-2 N or S protein antibodies as analytes and complete the entire assay within 20 minutes (incubation time in each step is 5 minutes). Conventional SARS-CoV-2 antibody ELISA involves a standard sandwich immunoassay format: immobilization of the antigen (recombinant S or N proteins) on the bottom of microtiter plate, capture of target antibodies, recognition and binding of biotinylated anti-human antibody and exposure to the streptavidin-HRP. In contrast to conventional antibody ELISA, plasmonic-fluor linked immunosorbent assay (p-FLISA) involves the use of plasmonic-fluor as the label (Figure 1). To determine the sensitivity and limit of detection (LOD, defined as mean + 3σ of the blank) of ELISA and p-FLISA in detecting the target antibodies, serially diluted anti SARS-CoV-2 N protein IgG solutions of known concentration (1 to 10^6 pg/ml) was first used as standards. In this 20-minute assay, LOD of p-FLISA was found to be 10 pg/ml, 440-fold lower than that of the ELISA (4.4 ng/ml) (Figure 2D). Similarly, the LOD of p-FLISA for anti-S protein RBD domain IgG was measured to be 411 pg/ml, which is 80-fold lower than that of conventional ELISA (30.6 ng/ml) (Figure 2E).

The remarkable brightness of plasmonic-fluor, while greatly improving the efficiency and detection limit of the assay, may result in higher background signal with even low non-specific binding, consequently compromising the specificity. To test the signal-to-noise ratio before and after applying plasmonic-fluor, we employed BSA coated wells as blank and streptavidin-CW800 coated wells as samples. The background signal increased with an increase in the concentration of plasmonic-fluor. However, the signal-to-noise ratio with plasmonic-fluor (OD of 0.5) is more than 170-fold higher than that of conventional

fluorophore. Using different concentration of plasmonic-fluor (OD values 0.5, 1, 1.5 and 2), the LOD of p-FLISA for SARS-CoV-2 S protein RBD domain antibody was measured at 411 pg/ml, 864 pg/ml, 1302 pg/ml and 1225 pg/ml, respectively, which are all substantially lower than that of antibody ELISA (30.6 ng/ml) (Figure S2). High concentration of plasmonic-fluor resulted in a slight increase in the background and, as a consequence, compromised the LOD of the assay. We have employed the plasmonic fluor with OD 0.5 in the following experiments.

To validate the performance of p-FLISA, we set out to detect SARS-CoV-2 antibodies in 10 plasma samples from PCR-confirmed COVID-19 positive patients collected after their recovery and a healthy control sample acquired before COVID-19 outbreak. We first measured and analyzed IgG targeting S protein subunit 1 and N protein using 20-minute p-FLISA. Fluorescence intensity corresponding to convalescent plasma samples is much higher than that of the healthy control sample (Figure 3A, 3B and S3). The levels of anti N protein IgG are significantly higher compared to anti-S protein subunit 1 IgG across all patients. Notably, owing to the high sensitivity of 20-min p-FLISA, anti N protein IgG in 9 out of 10 patient samples are still detectable even after more than 20,000-fold dilution (Figure S3 and S4). To further compare with the conventional FLISA, we measured and compared antibodies levels in serially diluted convalescent plasma from patient 13 using antibody FLISA and p-FLISA with different incubation durations in each step, from 5 minutes to 60 minutes. Fluorescence intensity obtained with plasmonic-fluor are 1900±200-fold higher compared to conventional fluorophore for different dilutions of plasma at each time point (Figure S5A). Moreover, fluorescence intensity in both assays demonstrate excellent linearity with assay time and dilution factor, suggesting accurate detection of IgG in patient plasma with as short as 5 minutes of incubation time with diluted patient plasma (Figure S5B and S5C).

The absolute and relative abundance of different subclasses and isotypes of antibodies reflect the infection course and clinical outcomes of the patient (detailed discussion can be found in SI). To evaluate the detection ability of multiple antibody isotypes, we employed plasma from patient 19 as a representative sample and measured isotype levels against viral antigens including S 1, S 2, and RBD domain of S protein and the N

protein using 20-minute FLISA and p-FLISA. Fluorescence intensity obtained after applying plasmonic-fluor successfully revealed the existence all isotypes targeting different viral antigens even at more than 1000-fold dilution (Figure S6). Conversely, conventional FLISA exhibited negligible fluorescence signals for all isotypes, except for the most robust immune response, IgG targeting N protein at 100-fold dilution (lowest dilution factor).

Detection of epitope-specific antibodies against SARS-CoV-2

The antigenic drift and consequent escape from current therapeutic interventions have been the major concerns of COVID-19. For example, mutations including the deletion in the NTD of S1 protein[17] have been reported to alter activity of neutralizing antibody.[18-20] In a previous study, two linear epitopes on spike protein of SARS-CoV-2 prototypes were found to elicit potent antibodies in convalescent plasma upon the infection[10-11],mostly for IgGs[18, 21-25] but also for IgA[24]. Epitope 1 (aa 553-570) nearby the receptor binding domain is specific to SARS-CoV-2, while epitope 2 (aa 809-826) encompassing the fusion peptide is highly conserved in generic coronavirus (Figure 1). Antibody depletion assays demonstrated that antibodies recognizing these two epitopes significantly contribute to patient neutralization capacities for COVID-19. Therefore, a simple and rapid epitope specific serology assay will be instrumental in answering vaccine efficacy, longevity of effective immunization and the natural coverage of vaccine-naive but infected individuals, particularly in case of SARS-CoV-2 variants by simply incorporating epitopes of the identified or future identified mutations.

To detect epitope specific SARS-CoV-2 antibodies, we employed BSA-peptides as the capture elements, instead of pristine whole S or N protein. To conjugate SARS-CoV-2 specific peptides to BSA, the peptide comprised of epitope sequence was appended with a triglycine spacer and a cysteine residue at the N terminal. These peptides were covalently bound on BSA via a bifunctional crosslinker with N-hydroxysuccinimide (NHS) and maleimide group at either ends, reactive to amines and sulfhydryls respectively (Figure 4A and S7). To compare the ability of 20-minute antibody FLISA and p-FLISA in the detection of epitope-specific IgG, we first employed serial diluted convalescent plasma as samples. The fluorescence signals obtained with conventional fluorophores

corresponding to both epitopes were identically weak and approaching the background noise, while the ones after applying plasmonic fluor exhibited an excellent dilution-dependent curve, with stronger immune response towards epitope 1 (Figure 4B). In contrast, the colorimetric signals acquired from conventional antibody ELISA exhibited a large deviation and merely demonstrate discernable signal at the lowest dilution factor (Figure 4C). To compare the immune response of different immunoglobulin isotypes and even subclasses, we evaluated the existence of epitope-specific IgG, IgA, and a subclass, IgA1, from 8 different patient samples through 20-minute p-FLISA PFLISA. Notably, the obtained fluorescence signal demonstrates that the overall immunoglobulin response of IgG is stronger than IgA in convalescent plasma (Figure S8A and S8B). Fluorescence signals for IgG indicate different profile of antibodies generated against these two epitopes, where patients 11, 13, 15, 16 and 18 demonstrate higher IgG amount targeting epitope 2 (Figure S8A). On the other hand, fluorescence signals obtained for IgA suggest that epitope 2 specific antibody is dominant in patient 11, 14, 15, and 18 (Figure S8B). Specifically, IgG in patient 14 exhibited high background binding to albumin, while low non-specific binding in case of IgA. P-FLISA also enabled the detection of epitope specific IgA1, a unique subclass of antibody, correlating with the amount of total IgA but with even lower background signal (Figure S8C).

In order to achieve multiplexed detection of epitope specific antibody, a spatial multiplexed dot blot assay was realized by spotting a 2 μl droplet of the two types of BSA-peptide conjugates within one well separately as the capture elements (Figure 5A). To investigate the feasibility of employing plasmonic-fluor in this multiplexed assay, we measured titer of epitope specific IgG in eight convalescent patient samples with serial dilution. Fluorescence signals of the two BSA-peptide dots demonstrate the expected dilution-dependence, indicating the existence of epitope-specific IgG (Figure 5C and S9). The fluorescence signal obtained from the rest of the well represents the amount of possible anti-BSA IgG, which was subtracted as the background from the fluorescence signal from the dots. Notably, the antibody titer calculated from the fluorescence intensity reveals the existence of IgG targeting both epitopes, except patient 11 and 13 where the amount of epitope 1-specific IgG are close to the heathy serum control (Figure 5B and S9). Different IgG titers also uncover the varying IgG profile targeting these two epitopes

and indicates distinct immunity acquired upon SARS-CoV-2 infection from patient-to-patient. This detailed information achieved by epitope specific serology assay could potentially help the precise identification of potential convalescent plasma donors and evaluation of vaccine efficacy in population scale.

Conclusion:

In summary, we have demonstrated an ultrasensitive SARS-CoV-2 epitope-specific serological test in a spatially-multiplexed manner through plasmonically-enhanced fluoroimmunoassay. Plasmonic-fluor, serving as the ultrabright fluorescence reporter, significantly improved the detection sensitivity compared to conventional fluorophores and enzyme-driven colorimetric assay. Specifically, the LOD of the antibody p-FLISA for SARS-CoV-2 is nearly 100-fold better compared to ELISA, completed in 20 minutes. The ultrasensitive detection of various antibody isotypes and epitope-specific antibodies provides more insightful and detailed information about the immune response after infection. Owing to its high sensitivity and specificity, plasmonically-enhanced epitope specific serology assay demonstrated here will be highly attractive to determine the ability of vaccines to cover potential immune epitopes, duration of the immunity, and epidemiological investigation of symptomatic patients and discover asymptomatic individuals. The ultrasensitive serology platform introduced here can be easily adapted to other infectious diseases by simply replacing the biodetection elements.

While the work presented here demonstrates the proof-of-concept of an ultrasensitive plasmon-enhanced serological assay for the detection of epitope-specific antibodies, further validation of the serological assay with larger number of control samples obtained from individuals without COVID-19 infection as well as vaccinated population are required before clinical translation. In addition, testing the assay with samples obtained from COVID-19 patients infected with different SARS-CoV-2 variants will further validate the generality of this epitope-specific serological assay and possible limitations.

Acknowledgements

We acknowledge support from National Science Foundation (CBET-2027145), National Cancer Institute-Innovative Molecular Analysis Technologies (R21CA236652), the National Cancer Institute (R01CA141521), and the Department of Anesthesiology of Washington University School of Medicine in St. Louis. The authors also thank Nano Research Facility (NRF) and Institute of Materials Science and Engineering (IMSE) at Washington University for providing access to electron microscopy facilities. The authors thank Dr. Qisheng Jiang and Dr. Jingyi Luan in Auragent Bioscience LLC for the preparation of plasmonic-fluor and application of dot blot assay.

Supporting information paragraph:

The Supporting Information is available free of charge on the ACS Publications website.

Additional experimental details, materials and results are included in Supporting information.

Competing interests

The authors declare the following competing financial interest(s): J.J.M., and S.S. are inventors on provisional patent related to plasmonic-fluor technology and the technology has been licensed by the Office of Technology Management at Washington University in St. Louis to Auragent Bioscience LLC. J.J.M., and S.S. are co-founders/shareholders of Auragent Bioscience LLC. J.J.M. and S.S. along with Washington University may have financial gain through Auragent Bioscience, LLC through this licensing agreement. These potential conflicts of interest have been disclosed and are being managed by Washington University in St. Louis.

Reference:

1. https://www.who.int/publications/m/item/weekly-epidemiological-update-on-covid-19---18-may-2021
2. Chen, R. E.; Zhang, X.; Case, J. B.; Winkler, E. S.; Liu, Y.; VanBlargan, L. A.; Liu, J.; Errico, J. M.; Xie, X.; Suryadevara, N., Resistance of SARS-CoV-2 variants to neutralization by monoclonal and serum-derived polyclonal antibodies. *Nature medicine* **2021**, 1-10.
3. Wang, Z.; Schmidt, F.; Weisblum, Y.; Muecksch, F.; Barnes, C. O.; Finkin, S.; Schaefer-Babajew, D.; Cipolla, M.; Gaebler, C.; Lieberman, J. A.; Oliveira, T. Y.; Yang, Z.; Abernathy, M. E.; Huey-Tubman, K. E.; Hurley, A.; Turroja, M.; West, K. A.; Gordon, K.; Millard, K. G.; Ramos, V.; Da Silva, J.; Xu, J.; Colbert, R. A.; Patel, R.; Dizon, J.; Unson-O'Brien, C.; Shimeliovich, I.; Gazumyan, A.; Caskey, M.; Bjorkman, P. J.; Casellas, R.; Hatziioannou, T.; Bieniasz, P. D.; Nussenzweig, M. C., mRNA vaccine-elicited antibodies to SARS-CoV-2 and circulating variants. *Nature* **2021**.
4. Khoury, D. S.; Cromer, D.; Reynaldi, A.; Schlub, T. E.; Wheatley, A. K.; Juno, J. A.; Subbarao, K.; Kent, S. J.; Triccas, J. A.; Davenport, M. P., Neutralizing antibody levels are highly predictive of immune protection from symptomatic SARS-CoV-2 infection. *Nature medicine* **2021**, 1-7.
5. Lew, T. T. S.; Aung, K. M. M.; Ow, S. Y.; Amrun, S. N.; Sutarlie, L.; Ng, L. F.; Su, X., Epitope-Functionalized Gold Nanoparticles for Rapid and Selective Detection of SARS-CoV-2 IgG Antibodies. *ACS nano* **2021**.
6. Whitman, J. D.; Hiatt, J.; Mowery, C. T.; Shy, B. R.; Yu, R.; Yamamoto, T. N.; Rathore, U.; Goldgof, G. M.; Whitty, C.; Woo, J. M., Evaluation of SARS-CoV-2 serology assays reveals a range of test performance. *Nature biotechnology* **2020,** *38* (10), 1174-1183.
7. Krammer, F.; Simon, V., Serology assays to manage COVID-19. *Science* **2020,** *368* (6495), 1060-1061.
8. Luchsinger, L. L.; Ransegnola, B. P.; Jin, D. K.; Muecksch, F.; Weisblum, Y.; Bao, W.; George, P. J.; Rodriguez, M.; Tricoche, N.; Schmidt, F., Serological assays estimate highly variable SARS-CoV-2 neutralizing antibody activity in recovered COVID-19 patients. *Journal of clinical microbiology* **2020,** *58* (12).
9. Shrock, E.; Fujimura, E.; Kula, T.; Timms, R. T.; Lee, I.-H.; Leng, Y.; Robinson, M. L.; Sie, B. M.; Li, M. Z.; Chen, Y., Viral epitope profiling of COVID-19 patients reveals cross-reactivity and correlates of severity. *Science* **2020,** *370* (6520).
10. Poh, C. M.; Carissimo, G.; Wang, B.; Amrun, S. N.; Lee, C. Y.-P.; Chee, R. S.-L.; Fong, S.-W.; Yeo, N. K.-W.; Lee, W.-H.; Torres-Ruesta, A., Two linear epitopes on the SARS-CoV-2 spike protein that elicit neutralising antibodies in COVID-19 patients. *Nature communications* **2020,** *11* (1), 1-7.
11. Amrun, S. N.; Lee, C. Y.-P.; Lee, B.; Fong, S.-W.; Young, B. E.; Chee, R. S.-L.; Yeo, N. K.-W.; Torres-Ruesta, A.; Carissimo, G.; Poh, C. M., Linear B-cell epitopes in the spike and nucleocapsid proteins as markers of SARS-CoV-2 exposure and disease severity. *EBioMedicine* **2020,** *58*, 102911.
12. Luan, J.; Seth, A.; Gupta, R.; Wang, Z.; Rathi, P.; Cao, S.; Gholami Derami, H.; Tang, R.; Xu, B.; Achilefu, S.; Morrissey, J. J.; Singamaneni, S., Ultrabright fluorescent nanoscale labels for the femtomolar detection of analytes with standard bioassays. *Nat Biomed Eng* **2020,** *4* (5), 518-530.
13. Luan, J.; Seth, A.; Gupta, R.; Wang, Z.; Rathi, P.; Cao, S.; Derami, H. G.; Tang, R.; Xu, B.; Achilefu, S., Ultrabright fluorescent nanoscale labels for the femtomolar detection of analytes with standard bioassays. *Nature biomedical engineering* **2020,** *4* (5), 518-530.

14. Lee, K.-S.; El-Sayed, M. A., Dependence of the enhanced optical scattering efficiency relative to that of absorption for gold metal nanorods on aspect ratio, size, end-cap shape, and medium refractive index. *The Journal of Physical Chemistry B* **2005,** *109* (43), 20331-20338.
15. Fischer, P. U.; Fischer, K.; Curtis, K. C.; Huang, Y.; Fetcho, N.; Goss, C. W.; Weil, G. J., Evaluation of commercial rapid lateral flow tests, alone or in combination, for SARS-CoV-2 antibody testing. *The American Journal of Tropical Medicine and Hygiene* **2021,** *105* (2), 378.
16. Lagerqvist, N.; Maleki, K. T.; Verner-Carlsson, J.; Olausson, M.; Dillner, J.; Byström, J. W.; Monsen, T.; Forsell, M.; Eriksson, J.; Bogdanovic, G., Evaluation of 11 SARS-CoV-2 antibody tests by using samples from patients with defined IgG antibody titers. *Scientific reports* **2021,** *11* (1), 1-8.
17. McCarthy, K. R.; Rennick, L. J.; Nambulli, S.; Robinson-McCarthy, L. R.; Bain, W. G.; Haidar, G.; Duprex, W. P., Recurrent deletions in the SARS-CoV-2 spike glycoprotein drive antibody escape. *Science* **2021,** *371* (6534), 1139-1142.
18. Lu, S.; Xie, X. X.; Zhao, L.; Wang, B.; Zhu, J.; Yang, T. R.; Yang, G. W.; Ji, M.; Lv, C. P.; Xue, J.; Dai, E. H.; Fu, X. M.; Liu, D. Q.; Zhang, L.; Hou, S. J.; Yu, X. L.; Wang, Y. L.; Gao, H. X.; Shi, X. H.; Ke, C. W.; Ke, B. X.; Jiang, C. G.; Liu, R. T., The immunodominant and neutralization linear epitopes for SARS-CoV-2. *Cell reports* **2021,** *34* (4), 108666.
19. Wang, L.; Wang, L.; Zhuang, H., Profiling and characterization of SARS-CoV-2 mutants' infectivity and antigenicity. *Signal Transduct Target Ther* **2020,** *5* (1), 185.
20. Wang, P.; Nair, M. S.; Liu, L.; Iketani, S.; Luo, Y.; Guo, Y.; Wang, M.; Yu, J.; Zhang, B.; Kwong, P. D.; Graham, B. S.; Mascola, J. R.; Chang, J. Y.; Yin, M. T.; Sobieszczyk, M.; Kyratsous, C. A.; Shapiro, L.; Sheng, Z.; Huang, Y.; Ho, D. D., Antibody Resistance of SARS-CoV-2 Variants B.1.351 and B.1.1.7. *Nature* **2021**.
21. Amrun, S. N.; Lee, C. Y.; Lee, B.; Fong, S. W.; Young, B. E.; Chee, R. S.; Yeo, N. K.; Torres-Ruesta, A.; Carissimo, G.; Poh, C. M.; Chang, Z. W.; Tay, M. Z.; Chan, Y. H.; Chen, M. I.; Low, J. G.; Tambyah, P. A.; Kalimuddin, S.; Pada, S.; Tan, S. Y.; Sun, L. J.; Leo, Y. S.; Lye, D. C.; Renia, L.; Ng, L. F. P., Linear B-cell epitopes in the spike and nucleocapsid proteins as markers of SARS-CoV-2 exposure and disease severity. *EBioMedicine* **2020,** *58*, 102911.
22. Li, Y.; Lai, D. Y.; Zhang, H. N.; Jiang, H. W.; Tian, X.; Ma, M. L.; Qi, H.; Meng, Q. F.; Guo, S. J.; Wu, Y.; Wang, W.; Yang, X.; Shi, D. W.; Dai, J. B.; Ying, T.; Zhou, J.; Tao, S. C., Linear epitopes of SARS-CoV-2 spike protein elicit neutralizing antibodies in COVID-19 patients. *Cell Mol Immunol* **2020,** *17* (10), 1095-1097.
23. Mishra, N.; Huang, X.; Joshi, S.; Guo, C.; Ng, J.; Thakkar, R.; Wu, Y.; Dong, X.; Li, Q.; Pinapati, R. S.; Sullivan, E.; Caciula, A.; Tokarz, R.; Briese, T.; Lu, J.; Lipkin, W. I., Immunoreactive peptide maps of SARS-CoV-2. *Commun Biol* **2021,** *4* (1), 225.
24. Shrock, E.; Fujimura, E.; Kula, T.; Timms, R. T.; Lee, I. H.; Leng, Y.; Robinson, M. L.; Sie, B. M.; Li, M. Z.; Chen, Y.; Logue, J.; Zuiani, A.; McCulloch, D.; Lelis, F. J. N.; Henson, S.; Monaco, D. R.; Travers, M.; Habibi, S.; Clarke, W. A.; Caturegli, P.; Laeyendecker, O.; Piechocka-Trocha, A.; Li, J. Z.; Khatri, A.; Chu, H. Y.; Collection, M. C.-.; Processing, T.; Villani, A. C.; Kays, K.; Goldberg, M. B.; Hacohen, N.; Filbin, M. R.; Yu, X. G.; Walker, B. D.; Wesemann, D. R.; Larman, H. B.; Lederer, J. A.; Elledge, S. J., Viral epitope profiling of COVID-19 patients reveals cross-reactivity and correlates of severity. *Science* **2020,** *370* (6520).
25. Wang, H.; Wu, X.; Zhang, X.; Hou, X.; Liang, T.; Wang, D.; Teng, F.; Dai, J.; Duan, H.; Guo, S.; Li, Y.; Yu, X., SARS-CoV-2 Proteome Microarray for Mapping COVID-19 Antibody Interactions at Amino Acid Resolution. *ACS Cent Sci* **2020,** *6* (12), 2238-2249.

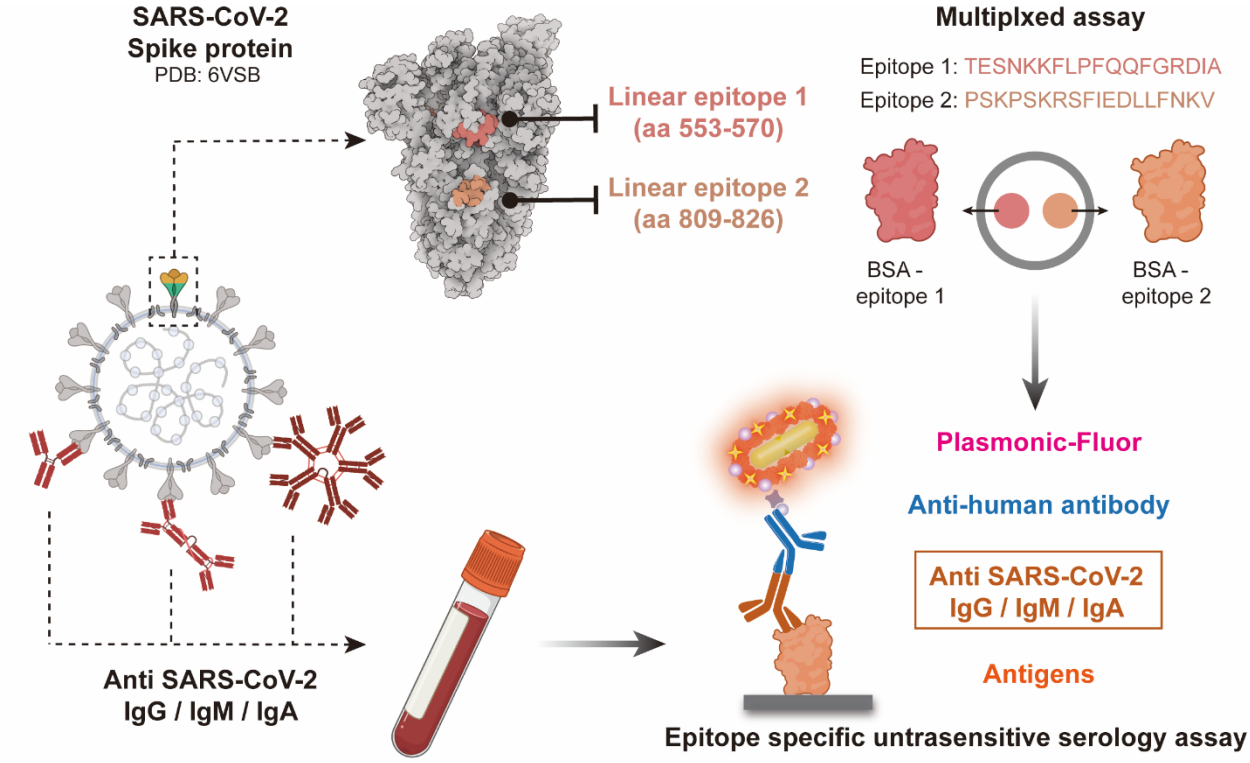

Figure 1. Schematic illustration of plasmonic-fluor enhanced epitope-specific SARS-CoV-2 serology assay in a multiplexed manner.

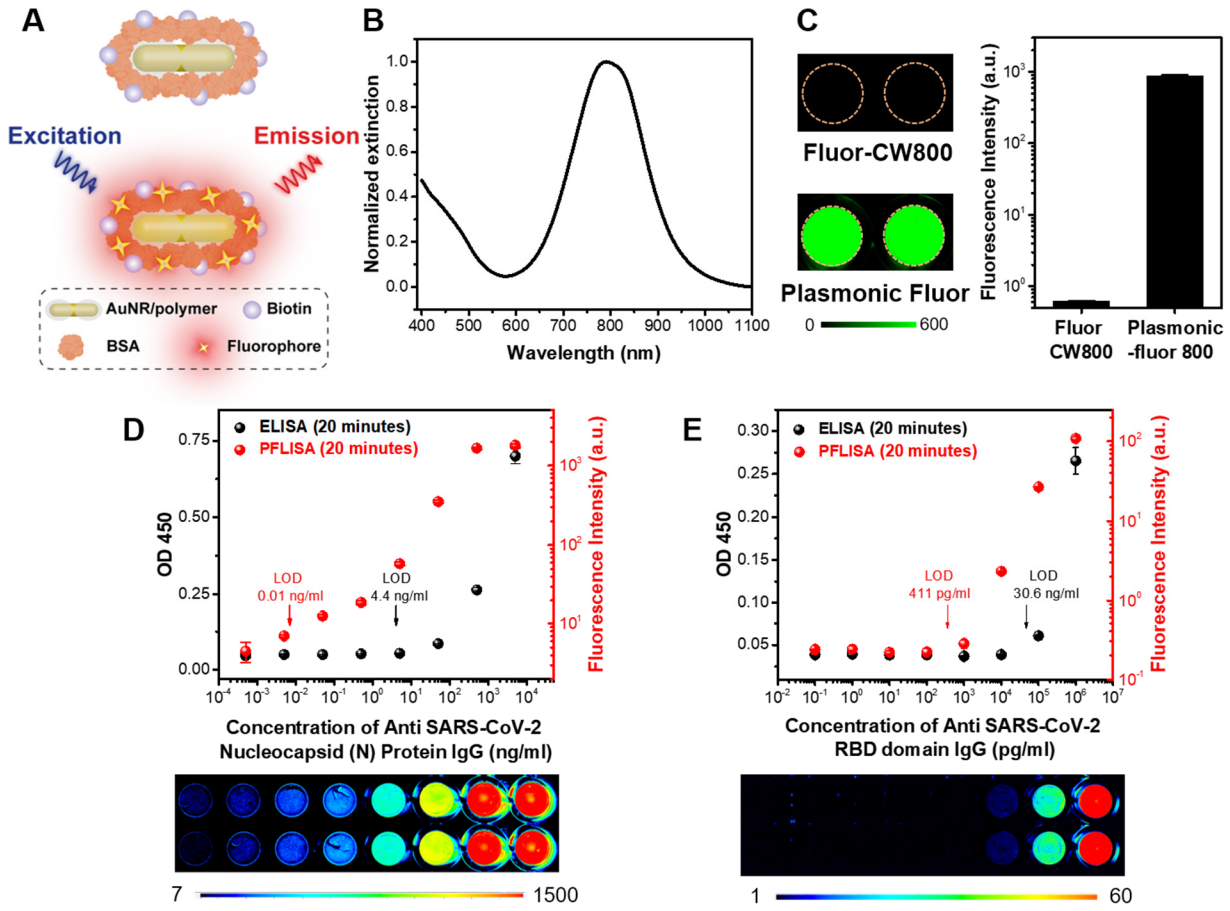

Figure 2. (A) Schematic illustration of plasmonic fluor as the ultrabright fluorescence nanolabel comprising of gold nanorod as plasmonic core, polymer spacer layer, fluorophores, and biotin, as the universal recognition element. **(B)** Visible-NIR extinction of plasmonic-fluor. **(C)** Fluorescence images and corresponding fluorescence intensity of streptavidin-CW800 before and after specific binding of plasmonic-fluor through interaction between biotin and streptavidin, showing a 1500-fold increased fluorescence intensity after applying plasmonic-fluor. Data are mean ± s.d. a.u., arbitrary units. **(D)** Dose-dependent fluorescence intensity anti SARS-CoV-2 Nucleocapsid (N) protein IgG on microtiter plate by conventional ELISA (black dots) and p-FLISA (red dots) performed in 20 minutes. Bottom image: Fluorescence intensity maps at various analytes concentration. **(E)** Anti SARS-CoV-2 spike protein RBD domain IgG dose-dependent fluorescence intensity on microtiter plate by conventional ELISA (black dots) and p-FLISA (red dots) performed in 20 minutes. Bottom image: Fluorescence intensity maps at various analytes concentration.

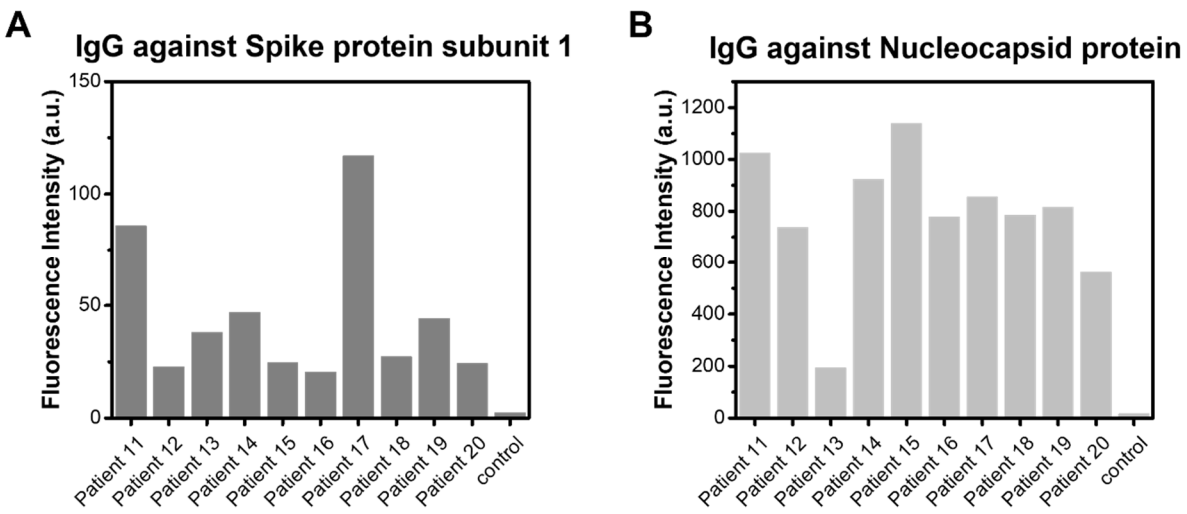

Figure 3. Fluorescence intensity obtained with plasmonic-fluor demonstrating IgG response targeting SARS-CoV-2 S protein subunit 1 **(A)** and N protein **(B)** in individual convalescent patient plasma and healthy control at 1/270 times dilution.

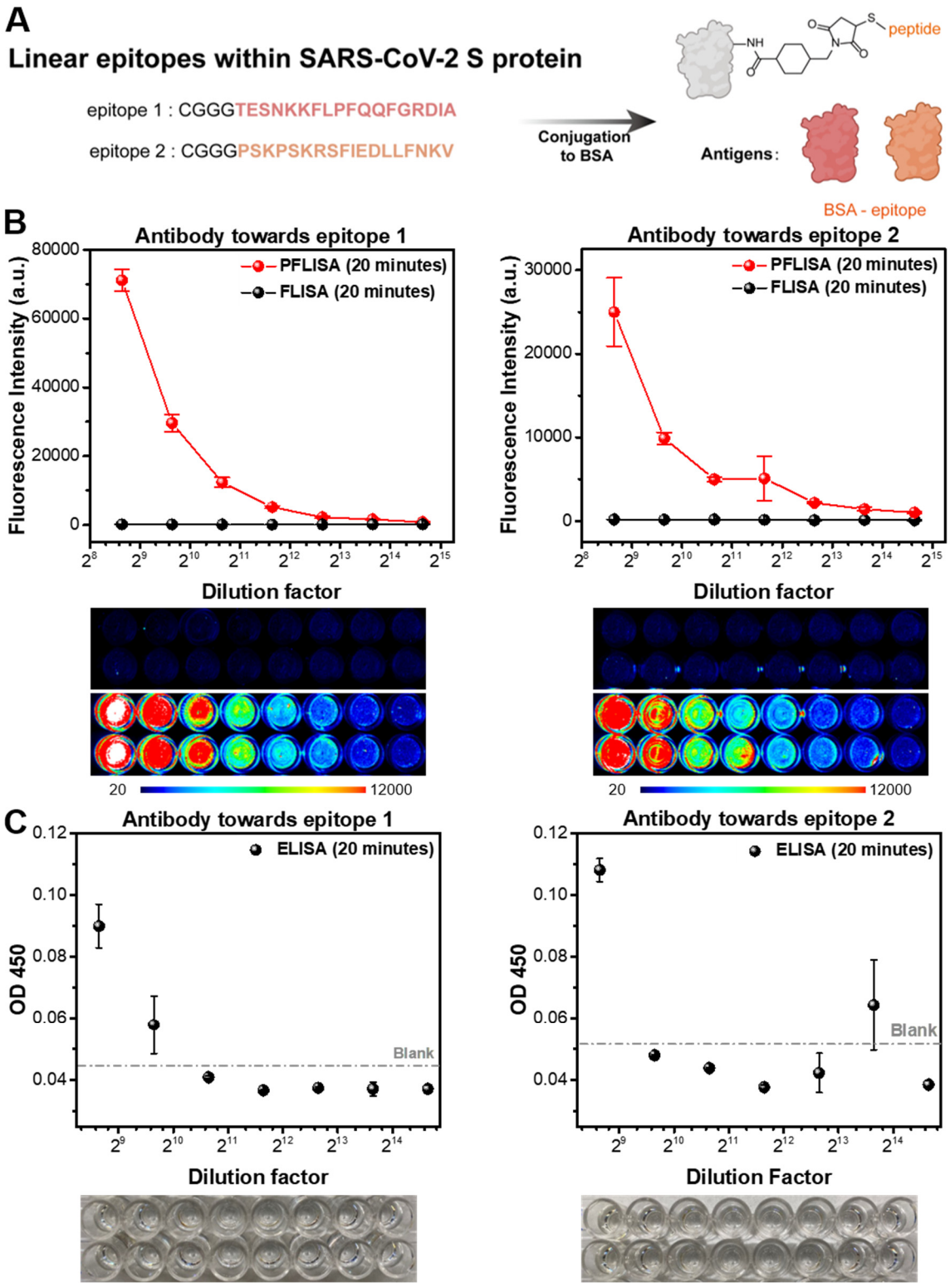

Figure 4. **(A)** Schematic illustration depicting the structure of peptides encoding the sequence of SARS-CoV-2 neutralization epitopes and their conjugations with BSA. A cysteine was added to allow coupling to the BSA scaffold along with three glycines to

project the peptide from the BSA surface. **(B)** Fluorescence intensity and intensity maps obtained before (black) and after (red) application of plasmonic-fluor, and **(C)** optical density and image of conventional ELISA with various dilution factor of convalescent patient plasma 17 (left) and patient 15 (right), respectively, demonstrating epitope 1 and 2 specific IgG. All the assays were accomplished in 20 minutes with 5 minutes incubation for each step.

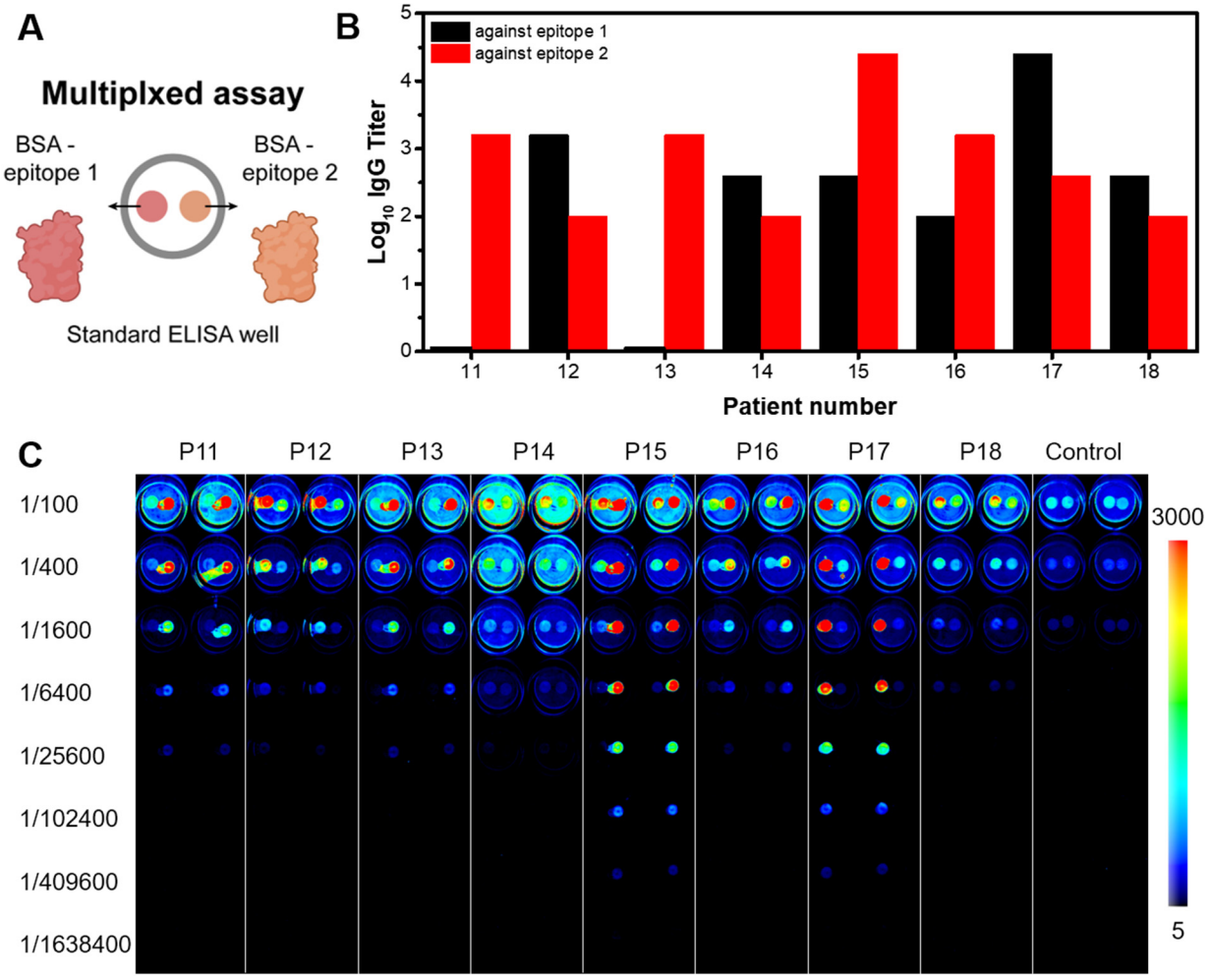

Figure 5. **(A)** Scheme illustrating arrangement of spatially multiplexed detection of epitope-specific antibodies. **(B)** Log_{10} titer of IgG in convalescent patient plasma targeting epitope 1 (black) and epitope 2 (red), measured by antibody p-FLISA. **(C)** Fluorescence intensity mapping after application of plasmonic-fluor showing the spatial multiplexed detection of IgG targeting different epitopes in individual convalescent patient plasma and healthy control.

For Table of Contents Only:

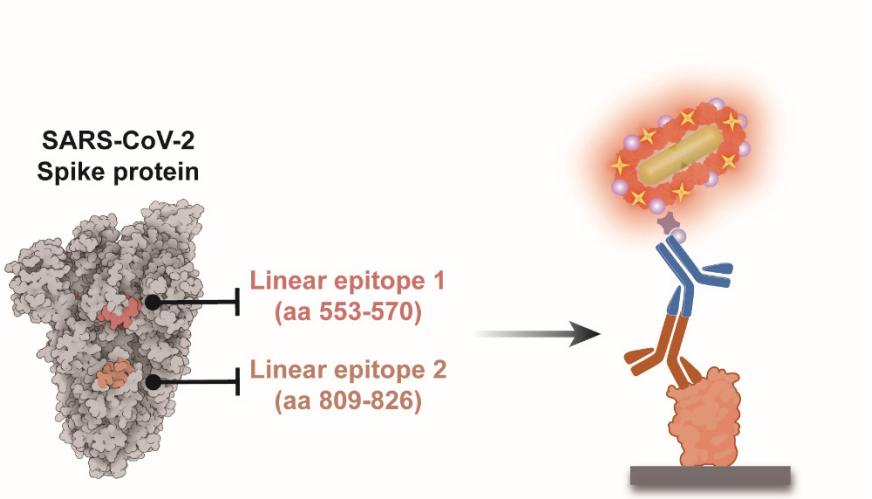

Epitope-specific and untrasensitive serology assay